International Journal of Thin Film Science and Technology

Volume 9
Issue 1 *Jan. 2020*

Article 7

2020

Analytical Modelling and Simulation of Highly Sensitive n-RADFET Dosimeter

Srijan Pathak
Department of Electronics & Communication Engineering. Motilal Nehru National Institute of Technology, Allahabad, India-211004., shtri@mnnit.ac.in

Spriha Singh
Department of Electronics & Communication Engineering. Motilal Nehru National Institute of Technology, Allahabad, India-211004., shtri@mnnit.ac.in

Tanya Jha
Department of Electronics & Communication Engineering. Motilal Nehru National Institute of Technology, Allahabad, India-211004., shtri@mnnit.ac.in

Ankush Agrawal
Department of Electronics & Communication Engineering National Institute of Technology Raipur, Chattisgarh, India- 492010., shtri@mnnit.ac.in

Shweta Tripathi
Department of Electronics & Communication Engineering. Motilal Nehru National Institute of Technology, Allahabad, India-211004., shtri@mnnit.ac.in

International Journal of Thin Films Science and Technology

http://dx.doi.org/10.18576/ijtfst/090107

Analytical Modelling and Simulation of Highly Sensitive n-RADFET Dosimeter

Srijan Pathak[1], *Spriha Singh*[1], *Tanya Jha*[1], *Ankush Agrawal*[2] *and Shweta Tripathi*[1*]

[1]Department of Electronics & Communication Engineering. Motilal Nehru National Institute of Technology, Allahabad, India-211004.
[2]Department of Electronics & Communication Engineering National Institute of Technology Raipur, Chattisgarh, India-492010.

Received: 2 Aug. 2019, Revised: 22 Nov. 2019, Accepted: 23 Nov. 2019

Published online: 1 Jan. 2020

Abstract: In the present paper, we have developed a model of a n-RADFET dosimeter device. Moreover, the study has addressed the effects of ionizing radiation on the surface potential and threshold voltage characteristics of the device. In addition, a detailed simulation analysis of the device has been conducted to obtain some further results. The study indicated that high sensitivity can be obtained for RADFET using n-MOSFET device. The results are expected to benefit in establishing the effectiveness of n-RADFET device as a dosimeter.
Keywords: — Dosimeter, High sensitivity, Ionizing radiation, MOSFET.

1 Introduction

MOSFETs find various applications in fabrication of digital integrated circuits, including microprocessors and memory devices. Because of their large packing density and improved robustness, thousands of MOSFETs can be easily fabricated on a memory chip. Furthermore, MOSFET device can be made with both p-type and n-type semiconductors resulting in possible fabrication of complementary pairs of MOS transistors that are used in designing CMOS logic devices for low static power consumption.

Recently, exploring the effects of ionizing radiation on MOSFETs has become important. In 1963, Blair, Peck, Brown and Smits first analysed the effects of ionizing radiation on transistors used in the Telstar Communication satellite[1]. At that time, it was thought that MOSFETs are less susceptible to damage due to radiation compared to BJTs, also, the former is a majority carrier device [2]. However, Hughes and Giroux contradicted this perspective [3].Studies have shown that exposure of a MOSFET to ionizing radiation dose greater than50krad (Si) may be destructive[4].Hence, it is significant to devise means for developing radiation hardened devices that are less susceptible to radiation damage. Thus, they are safely used for military and space applications[5]. We need to study the behaviour of a MOSFET in the presence of ionizing radiation and analyse the reasons for the possible deviations. Two primary degradation mechanisms for a MOSFET exposed to ionizing radiation are defined as follows [6]:

a. In the semiconductor substrate (Si in this case), excess electron-hole pairs are generated. Studies have shown that in steady state condition, this attains a constant value under constant exposure.
b. The effect of radiation in the SiO_2 layer can be understood based on the two following components, namely:
i. Build-up of trapped positive charges in the oxide layer.
ii. Increase in the number of interface traps at Si-SiO_2 interface.

Generation of electron-hole pairs in the bulk region causes a temporary damage in nature i.e. its effect can be seen only in the presence of ionizing radiation because the excess electron-hole pairs generated have a very small lifetime (in nanoseconds or even less). Then, they effectively recombine [9].

However, the other mechanism causes a permanent damage to the device. Excess electron-hole pairs are generated in the SiO_2 layer as well. They may recombine or transport within the oxide. The mobility of electrons in SiO_2 is much higher compared to the holes [10]. Hence, the electrons quickly move towards the contacts, while the holes cannot because

*Corresponding author E-mail: shtri@mnnit.ac.in

their transport is governed by a complex trap-hopping process. Some holes may get trapped in the oxide layer itself resulting in a net positive charge, while the others may move to the interface and create an interface trap.

During exposure to continuous radiation, the first mechanism influences device performance. Incident dose-rate governs the creation of excess carriers that change the surface potential of the device. However, this effect is temporary. The major factor causing the permanent changes that occur in a MOSFET when exposed to ionizing radiation is the trapping of holes in the silicon oxide layer and the generation of interface traps [11]. When the total dose is increased, the number of trapped positive charges and interface traps increases [12]. The relatively immobile holes cause a negative shift in the flat band voltage and a decrease in the threshold voltage of the device. Mobility of the charge carriers in the surface channel is also adversely affected.

So far, the major application of RADFET is realised by using a p-channel device because of contributions of fixed traps and switching traps in threshold voltage shift. Recently, it has been shown that n-RADFET can replace p-RADFET due to its higher ultimate sensitivity [8]. To date, p-RADFET has been the predominant dosimeter device used for research and applications [9]. Various pieces of literature address p-RADFET;

2 Device Structure

A schematic structure of the short channel n-MOSFET used for the analysis and simulation is shown in fig. 1, where L, and t_{ox} represent the gate length and thickness of the gate oxide, respectively. The x and y axes of the schematic structure are considered to be along the channel length and the channel thickness, respectively. The gate electrode of the short channel n-MOSFET is made up of gate material with work function $\emptyset$ deposited over length L. In the present work, polysilicon is the gate material. The p-type substrate is uniformly doped with doping concentration of N_a=1× $10^{13} cm^{-3}$. The source and drain region are doped with a doping concentration of $N_{S/D} = 1 \times 10^{20} cm^{-3}$ and the channel is doped with a doping concentration N_p=1× $10^{16} cm^{-3}$. The depth of the SiO_2 layer is 2 nm and the depth of the source and drain ends is 10 nm. The substrate is 10 nm below the source and drain end. The channel length is 60 nm and the length of source and drain ends is12 nm each.

Hence, the total length and depth of the short channel n-MOSFET used for our analysis are 84 nm and 22 nm, respectively, but that is not the case with n-RADFET.

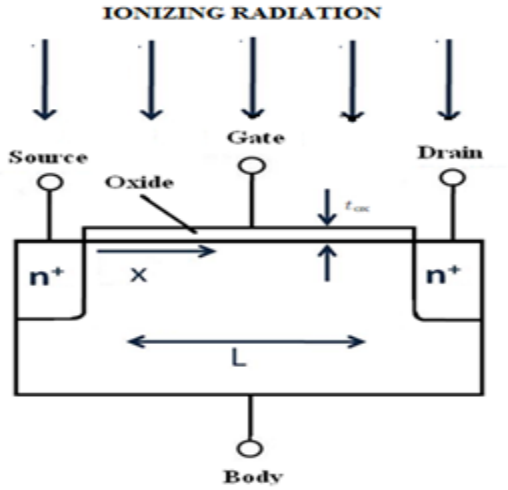

Fig.1: Structure of the device.

Keeping in mind that the high sensitivity of n-RADFET may establish it as a RADFET mainstream in the future, we have performed an in-depth theoretical analysis of n-RADFET.

In the present paper, we report a two-dimensional model for potential and threshold voltage of a n-channel MOSFET exposed to ionizing radiation. The results, based on the analytical model have been compared with the simulation results. Furthermore, in-depth simulation analysis of n-RADFET has been performed.

3 Theoretical Models

The 2D-channel potential $\emptyset(x,y)$ can be obtained in the channel region through solving two dimensional(2 D) Poisson's equation[15,16]

$$\frac{\partial^2 \emptyset(x,y)}{\partial x^2} + \frac{\partial^2 \emptyset(x,y)}{\partial y^2} = \frac{qN_a}{\epsilon_{si}} \quad (1)$$

where, ϵ_{si} is the permittivity of silicon and q is the charge of an electron .

The total carrier concentration N_a changes because of

ionizing radiation. It is written, as follows:

$$N_a=(n_{p_o}-p_{p_o})+(p_{p_o}+\Delta n)e^{-\beta\emptyset(x,y)}+(n_{p_o}+\Delta n)e^{(\beta\emptyset(x,y)-\beta V_d)} \quad (2)$$

n_{p_o} and p_{p_o} are thermally generated electron and hole concentration respectively and $\beta={}^{q}/_{kT}$; q is the electronic charge, k is the Boltzmann constant and T is the temperature .

Δn is the excess electron carrier generated in the depletion region and V_d is the applied drain voltage. Here Δn depends on the dose rate to which it is related by the given relation [13]:

$$\Delta n = g_o D^r \tau \quad (3)$$

where, g_o is the carrier generation rate conversion factor (carrier m^2 rad), D^r is the incident dose rate (rad $s^{-1}m^{-2}$) and τ is the lifetime of the carrier .

The boundary conditions used to solve the Poisson's equation are given as follows [14]

Boundary condition 1:

$$\frac{d\emptyset(x,y)}{dy}|_{y=0}=\frac{\epsilon_{ox}}{\epsilon_{si}}\left(\frac{\emptyset(x,y)-V_{gsn}}{t_f}\right) \quad (4)$$

Where ϵ_{ox} is the permittivity of the silicon dioxide, $\emptyset(x,y)$ is the surface potential of the region and V_{gsn} is the gate source voltage after exposure to the radiation.

The ionizing radiation creates build-up in the fixed oxide charge and a change in the interface state charge resulting in a change in the flat band voltage .Let V_{fb} be the flat band voltage without ionizing radiation ,

$$V_{fb}=\emptyset_m-\left(\gamma_{si}+\frac{E_g}{2*q}+V_t*\log\frac{N_a}{n_i}\right) \quad (5)$$

Where $\emptyset_m$ is the gate material work function of the region, γ_{si} is the electron affinity of silicon, E_g is the bandgap of silicon, n_i is the intrinsic carrier concentration of silicon .

Due to radiation change in flatband voltage can be written as follows:

$$\Delta V_{fb}=\frac{q}{C_{ox}}(\Delta N_{it}-\Delta N_{ot}) \quad (6)$$

Using V_{fb} and ΔV_{fb}, V_{gsn} can be given as follows,

$$V_{gsn}=V_{gs}-V_{fb}-\Delta V_{fb} \quad (7)$$

Boundary condition 2: The potential at the source-channel interface can be given as,

$$\emptyset(0,0)=V_{bi} \quad (8)$$

where V_{bi} is the built-in potential of the single gate single material MOSFET

Boundary condition 3: The potential at the source-channel interface can be given as follows,

$$\emptyset(L,0)=V_{bi}+V_{ds} \quad (9)$$

Where, V_{ds} is the effective drain source potential.

Boundary condition 4: The electric flux at the interface of buried oxide and the back channel is continuous

$$\frac{d\emptyset(x,y)}{dy}|_{y=t_{si}}=\frac{\epsilon_{ox}}{\epsilon_{si}}\left(\frac{V'_{sub}-\emptyset_b(x)}{t_b}\right) \quad (10)$$

where, t_b is the buried oxide thickness

V_{sub}= substrate bias

V_{fb} = Back channel flatband voltage

$$V'_{sub}=V_{sub}-V_{fb,b} \quad (11)$$

Now, the solution of Eq. (1) can be approximated as follows:

$$\emptyset(x,y)=\emptyset_s(x)+a_1(x)y+a_2(x)y^2 \quad (12)$$

Where

$$a_1(x)=\frac{\epsilon_{ox}}{\epsilon_{si}}\left[\frac{\emptyset_s(x)-V_{gsn}}{t_f}\right] \quad (13)$$

$$a_2(x)=\frac{-\epsilon_{ox}}{2\epsilon_{si}h(x)}\left[\frac{\emptyset_s(x)-V_{gsn}}{t_f}\right] \quad (14)$$

Let y=y_o where y_o is a constant value and $\emptyset_c(x)$ is the channel potential at y=y_o . Placing $a_1(x)$, $a_2(x)$ and y=y_o in equation(11) , we get

$$\emptyset_c(x)=\emptyset_s(x)+\frac{\epsilon_{ox}}{\epsilon_{si}}\left[\frac{\emptyset_s(x)-V_{gsn}}{t_f}\right]y_o-\frac{\epsilon_{ox}}{\epsilon_{si}}\left[\frac{\emptyset_s(x)-V_{gsn}}{t_f}\right]\frac{1}{2h(x)}y_o^2 \quad (15)$$

On solving equation (11), we get

$$\emptyset_s(x)=\emptyset_c(x)[1+\frac{\epsilon_{ox}}{\epsilon_{si}}\frac{y_o}{t_f}-\frac{\epsilon_{ox}}{\epsilon_{si}}\frac{y_o^2}{2h(x)}]^{-1}+\frac{[\frac{\epsilon_{ox}}{t_{si}}\frac{V_{gsn}y_o}{t_f}-\frac{t_{ox}y_o^2}{2t_{si}t_fh(x)}]}{[1+\frac{\epsilon_{ox}y_o}{\epsilon_{si}t_f}-\frac{\epsilon_{ox}y_o^2}{2\epsilon_{si}t_fh(x)}]} \quad (16)$$

Solving the Poisson's Equation at point y=y_o , we get

$$\frac{d^2\emptyset_c(x)}{dx^2}=\frac{1}{\lambda^2}[\emptyset_c(x)+\frac{\lambda^2qN_a-\epsilon_{si}(V_{gsn}-V_{fbn})}{\epsilon_{si}}] \quad (17)$$

Where

$$\lambda=\frac{\sqrt{t_{si}^2(4\epsilon_{si}t_{ox}+\epsilon_{ox}t_{si})}}{\sqrt{2\epsilon_{ox}t_{si}}} \quad (18)$$

Now, a generalised solution can be as follows:

$$\emptyset_c(x)=Ae^{\eta x}+Be^{-\eta x}-{}^{\beta}/_{\alpha} \quad (19)$$

$$\eta={}^{1}/_{\lambda}=\sqrt{\alpha} \quad (20)$$

$$\beta 1=1\frac{\lambda^2qN_a-\epsilon_{si}[V_{gsn}-V_{fbn}]}{\lambda^2\epsilon_{si}} \quad (21)$$

In conjunction with the boundary conditions equation (3) is solved to get,

$$A=V_{bi}-{}^{\beta}/_{\alpha}-B \quad (22)$$

In addition,

$$B=\frac{1}{(e^{-\eta^2}-e^{\eta^2})}[V_{bi}(1-e^{\eta^2})+V_{DS}+\frac{\beta}{\alpha}(1-e^{\eta^2})] \quad (23)$$

By Eqs. (11) , (15) , (18) , (21) and (22) the channel potential can be given by ,

$$\emptyset(x,y)=4[4\,\epsilon_{si}\,t_{ox}+2\,\epsilon_{ox}\,y_o]^{-1}\left[Ae^{\eta x}+Be^{-\eta x}-\frac{\beta}{\alpha}+\frac{\epsilon_{ox}y_o}{2\epsilon_{si}t_{ox}}(V_{gsn}-V_{fbn})\right]\left[\frac{2\epsilon_{si}y_ot_{ox}+2\epsilon_{ox}y_oy-\epsilon_{ox}y^2}{2y_o}\right]-\frac{\epsilon_{ox}(V_{gsn}-V_{fbn})}{\epsilon_{si}t_{ox}}[y-y^2(2y_o)^{-1}] \quad (24)$$

Under the threshold condition, the gate should be turned on to establish the conducting channel between the

source and the drain.

If $\emptyset_{c,min} = \emptyset_c(x)|_{x=x_{0,min}}$ represents the minimum middle channel potential then the distance, $x = x_{o,min}$ can be obtained by putting

$$\frac{d\emptyset_c(x)}{dx} = 0 \quad (25)$$

From the above-mentioned, $x_{0,min}$ can be obtained by $x_{o,min} = \frac{1}{2\eta}\ln\frac{B}{A}$

By Eq. (17) and Eq. (25) we get,

$$\phi_{c,min} = 2(AB)^{\frac{1}{2}} - qN_a\lambda^2{\epsilon_{si}}^{-1} + V_{gsn} - V_{fbn} \quad (26)$$

where $V_{fbn} = V_{fb} + \Delta V_{fb}$

The threshold voltage of the MOSFET is the gate voltage at which $\phi_{c,min} = 2\phi_f$ where $\phi_f = (\frac{kT}{q})\ln\frac{N_a}{n_i}$.Upon solving with the above -mentioned condition the expression of threshold it is given by,

$$V_T = \frac{2kT}{q}\ln\frac{N_a}{n_i} + qN_a\lambda^2{\epsilon_{si}}^{-1} - 2(AB)^{\frac{1}{2}} + V_{fbn} \quad (27)$$

4 Results and Discussion

Analytical modelling has been verified for short channel n-MOSFET by utilizing ATLAS simulator tool. The complete study is performed by considering n-MOSFET under ionizing radiation. The modelling initiates with the solution of two-dimensional Poisson's equation in the channel region. In continuation to the solution of Poisson's equation, the surface potential and threshold voltage for n-MOSFET were calculated under ionizing radiation. The surface potential is later used to define the influence of ionizing radiation on n-MOSFET with respect to the gate length. In fig. 2 we have demonstrated surface potential against the gate length with the variation of ionizing radiation dose rate. At any particular dose rate, the graph demonstrates the parabolic variation of channel potential against the length of gate. This is explained with the help of quadratic equation of surface potential illustrated by analytical modeling. Moreover, the effect on n-MOSFET surface potential can be observed by changing the dose rate over the entire area of MOSFET from 84 rad sec^{-1} to 252 rad sec^{-1} and then to 336 rad sec^{-1}. On increasing the dose rate the surface potential diminishes and the parabola shifts downwards. The effect depends on the total dose received by the device. As reported earlier, there are three mechanism of the exposure of ionizing radiation: it increases the holes traps at the oxide-substrate interface (commonly SiO_2-Si interface); builds up the oxide trapped charges and the excess electron gets accumulated in the inversion region. The net effect of all three mechanisms results in the increment of flat band voltage of the device. The decrease in the surface potential with an increase in dose rate occurs because of the cumulative effect of the mechanisms associated with ionizing radiation.

Fig.3 depicts the plot of threshold voltage against the gate length, with and without the introduction of ionizing radiation. Under pre-irradiated condition, on increasing the length of gate up-to 1 nm threshold voltage increases. However, after further increment it tends to saturate. This change occurs because of the elevation of the tiniest potential on increasing the gate length, which further causes a noteworthy reduction in the channel barrier up-to some extension and increases threshold voltage up-to some gate length. The similar control of gate length is detected on the threshold voltage under post-irradiated circumstances but with the left shifted graph involving higher values. This happens as a result of the hole traps in the oxide (SiO_2) of n-MOSFET. Conduction of current in conventional n-MOSFET occurs when channel inversion is created under external positive voltage V_{GS}. However, n-MOS device under the influence of ionizing radiation already has positive trapped holes in the oxide layer that attracts electrons from the p-substrate. Thus, in such cases, less V_{GS} is required to build an inversion layer and under high dose rate zero V_{GS} is required for the conduction. Hence, the threshold voltage gets shifted to the left. Zero V_{GS} and high dose rate case generate false conduction and are unfavorable. Consequently, selective ionizing dose rate has to be created for high sensitive applications.

The surface potential for the duration of exposure is expressed by the entire dose occupied by the device along with the ionizing radiation dose rate to which the n-MOS device is exposed. The significance of dose rate over the surface potential of the MOS device for the given gate voltage is represented in Fig.4. The plot reveals a remarkable decrement in the surface potential with an increment in the incident ionizing radiation dose rate for the specified gate voltage V_{GS}. Thus a substantial variation in the surface potential that may create an adverse result in the performance of the device.

From Fig. 2 to Fig. 4 all simulated data are compared with their mathematical results. Both results were in good agreement with each other. In Fig. 5 we have portrayed the modification in drain current with gate voltage. When V_{GS} is greater than the threshold voltage the drain current escalates suddenly to the highest value. In post-irradiated condition, the high value of threshold voltage causes declination in the drain current at higher dose rate of n-MOS device.

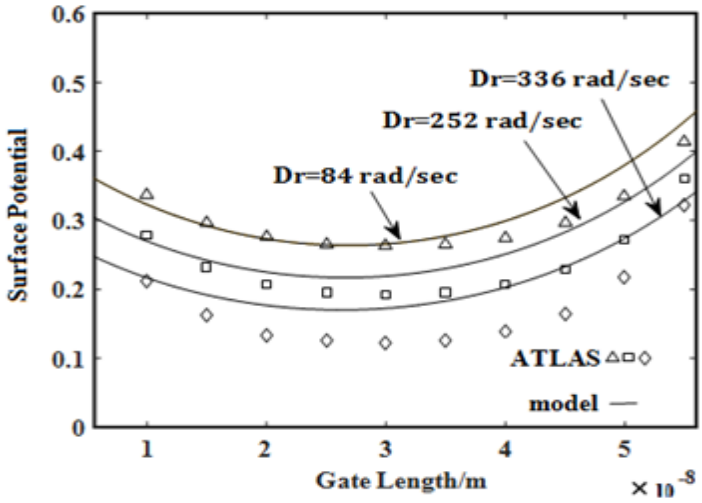

Fig.2: Plot of surface potential versus gate length under the exposure of different dose rate.

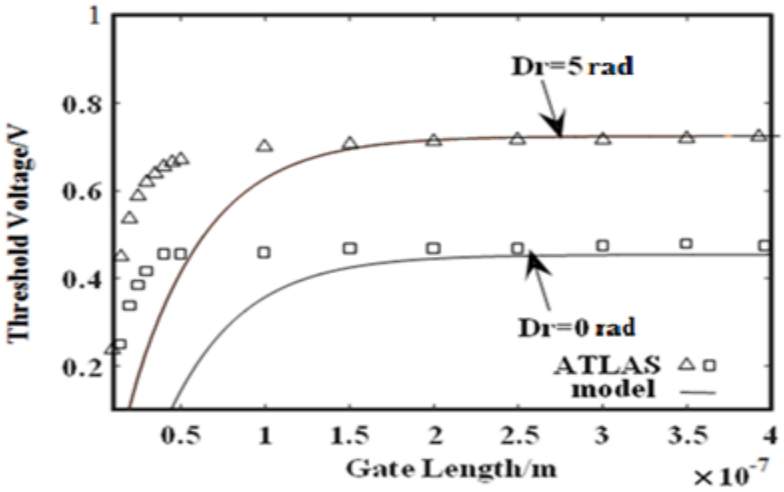

Fig.3: Plot of threshold potential versus gate length under preradiated and post radiated conditions.

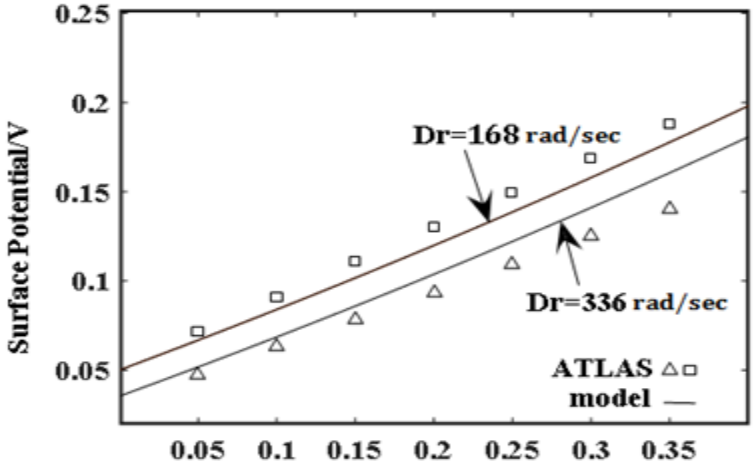

Fig. 4: Plot of surface potential versus gate to source voltage under the exposure of different dose rate.

Fig. 6 illustrates the alteration of drain current with respect to the drain voltage for both pre-irradiated and post irradiated situations of n-MOS device. Figure demonstrates that drain current increases up-to V_{DS}=0.4 volts and starts to saturate after 0.4V. In post-irradiated condition, under Saturation region the drain current decreases on increasing the dose rate. This occurs because of the decrement in charge carrier mobility along with the variation in the surface potential.

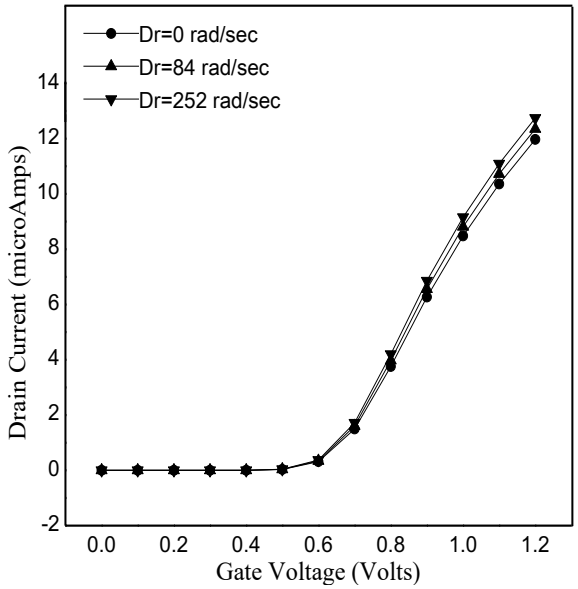

Fig. 5: Plot of drain current versus gate to source voltage under the exposure of different dose rate.

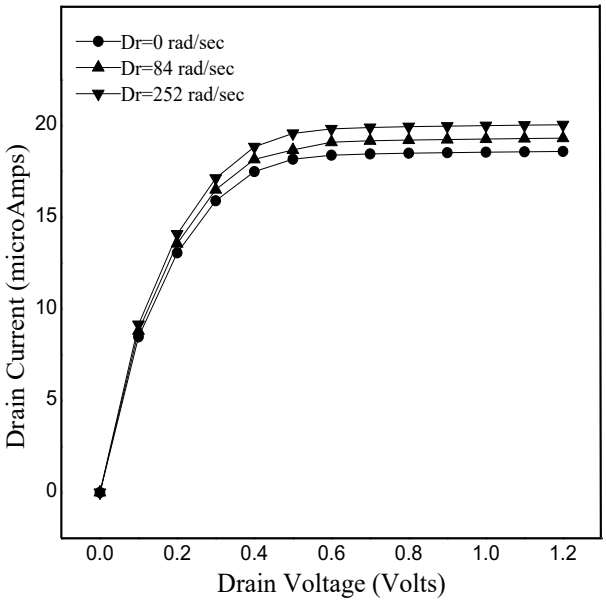

Fig. 6: Plot of drain current versus drain to source voltage under the exposure of different dose rate.

As discussed earlier, it can be seen numerically that on increasing the gate length, the threshold voltage increases. Under exposure the value of threshold voltage also rises. However, the opposite situation occurs in the case of sub-threshold voltage. Fig .7 exhibits the threshold voltage rolloff for dose rate 5 without any gate to source bias. It also depicts that the threshold voltage roll off remains constant throughout the gate length. Both the modeling and simulation results have been plotted. Furthermore, that the threshold voltage increases till certain gate length then, it tends to saturate explaining the behavior of threshold roll off for the post irradiated condition.

Table 1: Effect of gate length at threshold voltage and sub-threshold voltage under the exposure of different dose rate.

GATE LENGTH (nm)	V_t(Dose Rate=0) (volts)	V_t(Dose Rate=6) (volts)	Sub V_t(Dose Rate=0) (volts)	Sub V_t(Dose Rate=6) (volts)
10	0.23674	0.299546	0.813325	0.693368
15	0.449031	0.473262	0.266704	0.251434
20	0.535917	0.551984	0.157358	0.153972
25	0.586023	0.598313	0.123317	0.121643
30	0.617933	0.628038	0.106688	0.105971
35	0.639162	0.647877	0.098213	0.097842
40	0.65374	0.661522	0.093314	0.0931005
45	0.664065	0.671197	0.090274	0.0901422
50	0.671621	0.67828	0.088308	0.0882239
100	0.699082	0.703909	0.0841893	0.0841783
150	0.706925	0.711114	0.0838431	0.0838281
200	0.710727	0.71458	0.0837004	0.083696
300	0.714446	0.717946	0.0835074	0.083523
400	0.716269	0.719541	0.083421	0.083435

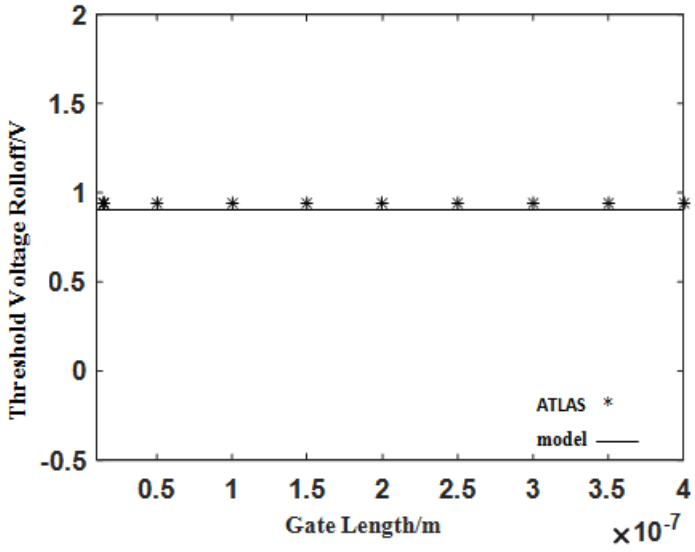

Fig. 7: Plot of threshold roll off versus gate length for dose rate=5.

Fig .8 shows the threshold voltage shift ΔV_T for radiation dose D in the range 0 to 200 rad without any gate bias($V_{gs} = 0$). The sensitivity of the RADFET is defined as the ratio between the voltage shift and the dose received ($\Delta V_T/D$).It also indicates that sensitivity for this particular device shows good linearity along with considerably high value, so it will be appropriate to be used as dosimeter. Accordingly, sensitivity in this case is 0.0181 V/radA comparative analysis of the sensitivity values of several studies is presented in a tabular form (Table 2) as follows:

The comparison exhibits that the sensitivity of our device is relatively higher. This highly sensitive n-channel dosimeter may find numerous applications in nuclear industry, radiotherapy for curing cancer and space related researches.

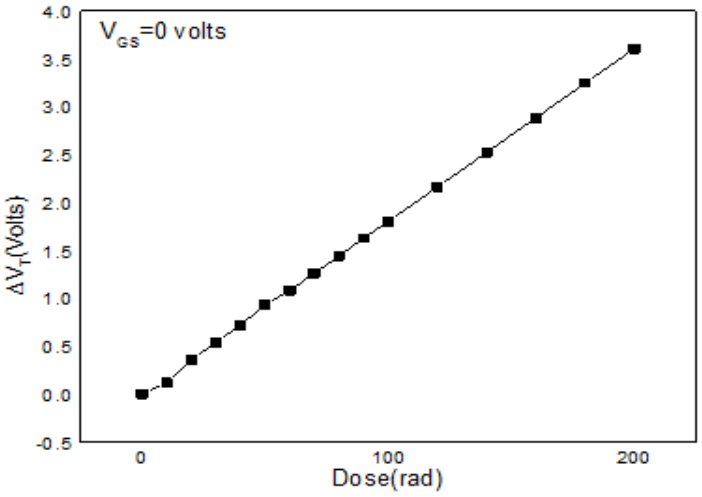

Fig. 8: Plot of threshold voltage shift versus dose for zero gate bias.

Table 2: Comparison of present work with some reported literatures

Reference	Value of Sensitivity	Sensitivity obtained from this study
Pejovic Milic et al. [17]	For t_{ox}=1 µm sensitivity= 2.9 mV/cGy	For t_{ox}= 0.001 µm and zero gate bias,sensitivity= 18.1 mV/cGy
Datasheet [18]	For t_{ox}= 0.3 µm, at zero gate bias Sensitivity=0.2 mV/cGy	
Asensio L.J. et al.[19]	Mean sensitivity value= 0.292 mV/cGy	

5 Conclusions

In the present paper, the 2D channel potential has been modelled for the n-RADFET dosimeter with high sensitivity using the parabolic approximation method. The behaviour of the surface potential with varying gate length and surface potential with V_{gs} at different dose rate has also been obtained. Furthermore, the behaviour of threshold voltage with different dose rate has been obtained . Moreover, with application of ionizing dose, a shift occurs in the threshold voltage. The sensitivity of the device has been calculated using the plot of threshold shift versus incident dose. Accordingly, the value of sensitivity is 18.1mV/cGy for the device with gate thickness of0.001 µm at zero gate bias (i.eVgs = 0V).

References

[1] Mitchell J P, Wilson D K. A Summary Effects of Radiation on Semiconductor Devices. No. scientific-1. Western electric co inc new York., 1965.

[2] Brown W L, GabbeJ D, and RosenzweigW. Results of the Telstar radiation experiments. Bell System Technical Journal., **42(4)**, 1505, 1963.

[3] Ma T P, Dressendorfer P V. Ionizing radiation effects in MOS devices and circuits. John Wiley & Sons., 1989.

[4] Tokuhiro A T, Bertino M F. Radiation resistance testing of MOSFET and CMOS as a means of risk management. IEEE Transactions on Components and Packaging Technologies., **25(3)**, 519, 2002.

[5] Chauhan R K, Dasgupta S, Chakrabarti P. A pseudo-two-dimensional model of an n-channel MOSFET under the influence of ionizing radiation. Semiconductor science and technology., , 17(9), 961, 2002.

[6] Pejovic M M. P-channel MOSFET as a sensor and dosimeter of ionizing radiation. FactaUniversitatis, Series: Electronics and Energetics., **29(4)**, 509, 2016.

[7] Zheng Y, Shi W, Wang M, et al. N-RADFET will able to replace P-RADFET.International Journal of Applied Research., **2(5)**, 958, 2016.

[8] Pejović M M, Pejović S M. VDMOSFET as a prospective dosimeter for radiotherapy. Applied Radiation and Isotopes., **132**, 1, 2018.

[9] Pejović M, et al. Influence of ionizing radiation and hot carrier injection on metal-oxide-semiconductor transistors. Current Topics in Ionizing Radiation Research. IntechOpen., 2012.

[10] Curtis Jr O L, Srour J R, Chiu K Y. Hole and electron transport in SiO2 films. Journal of Applied Physics., **45(10)**, 4506, 1974.

[11] Oldham T R, McLean F B. Total ionizing dose effects in MOS oxides and devices. IEEE transactions on nuclear science., **50(3)**, 483, 2003.

[12] Vasudevan V, Vasi J. A numerical simulation of hole and electron trapping due to radiation in silicon dioxide. Journal of applied physics., **70(8)**, 4490, 1991.

[13] Larin F. Radiation Effects in Semiconductor Devices, New York: Wiley., 1968.

[14] Reddy G V, Kumar M J. A new dual-material double-gate (DMDG) nanoscale SOI MOSFET-two-dimensional analytical modeling and simulation. IEEE Transactions on Nanotechnology., **4(2)**, 260, 2005.

[15] Young K K. Short-channel effect in fully depleted SOI MOSFETs. IEEE Transactions on Electron Devices., **36(2)**,399, 1989.

[16] Tripathi S. A two-dimensional analytical model for channel potential and threshold voltage of short channel dual material gate lightly doped drain MOSFET. Chinese Physics B., **23(11)**, 118505, 2014.

[17] Pejović M, et al. Sensitivity of P-channel MOSFET to X-and gamma-ray irradiation. International Journal of Photoenergy,, 2013.

[18] REM Low-Fade Silicon MOSFET Dosimeter.Data sheet: Type RFT300-CC10G1, 2010.

[19] Brown W L, Gabbe J D, Rosenzweig W. Results of the Telstar radiation experiments. Bell System Technical Journal,, **42(4)**, 1505, 1963.